

**Enhancement of the oxidative removal of diclofenac and of the  $\text{TiO}_2$  rate of photon absorption in dye-sensitized solar pilot scale CPC photocatalytic reactors**

*Diaz-Angulo, Jennyfer<sup>1</sup>, Lara-Ramos, Jose<sup>1</sup>, Mueses, Miguel<sup>2</sup>, Hernández-Ramírez, Aracely<sup>3</sup>, Li Puma, Gianluca<sup>4</sup>, Machuca-Martínez, Fiderman<sup>1</sup>*

*<sup>(1)</sup>Grupo GAOX, Escuela de Ingeniería Química, Universidad del Valle, Cali, Colombia.*

*<sup>(2)</sup>Photocatalysis and Solar Photoreactors Engineering, Department of Chemical Engineering, Universidad de Cartagena, Cartagena, Colombia,*

*<sup>(3)</sup>Facultad de Ciencias Químicas, Universidad Autónoma de Nuevo León. San Nicolas de los Garza, México.*

*<sup>(4)</sup>Environmental Nanocatalysis & Photoreaction Engineering, Department of Chemical Engineering, Loughborough University, Leicestershire, UK*

**\* Corresponding author:** [fiderman.machuca@correounivalle.edu.co](mailto:fiderman.machuca@correounivalle.edu.co) *Escuela de Ingeniería Química, Universidad del Valle, Cali, Colombia*

**Abstract**

The sensitization of rate of photon absorption of a  $\text{TiO}_2$  photocatalyst irradiated by natural solar radiation in pilot scale compound parabolic collectors (CPC's) photoreactors was investigated. Methyl red (MR) dye was used as a photo-sensitizer to increase the rate of photon absorption of a  $\text{TiO}_2$  photocatalyst and the oxidative removal of the common pharmaceutical diclofenac (DCF) in solar, pilot scale, compound parabolic collectors (CPC's) pho-

toreactors. The impact of the concentrations of  $\text{TiO}_2$  and MR were investigated and tuned to determine the most effective operational conditions. The results show that the dye-sensitization process of the catalyst and the degradation of DCF were favored at catalyst concentrations close to the optimum. Complete degradation and mineralization of DCF were achieved under most effective operational conditions. The mineralization of DCF and dye increased by up to 65% in the presence of the MR sensitizer compared to the results without sensitizer. The oxidation by-products formed during the process were identified by gas chromatography–mass spectrometry (GC–MS). A detailed mechanism of the dye-sensitization process was proposed, and a kinetic model for the simultaneous degradation of diclofenac and the dye was derived using the pseudo-stationary state method. This study demonstrates the positive impact of dye sensitizers on the photocatalytic degradation of pharmaceuticals in pilot scale photoreactors irradiated by natural sunlight

**Keywords:** Dye-sensitized; Visible light; photon absorption; solar radiation; pilot scale reactor; Methyl Red.

## 1. Introduction

In recent years, the treatment and removal of micropollutants from water and wastewater have been increasingly investigated due to the adverse effects these species may pose to the environment and to human health. Among these pollutants, pharmaceutical compounds and their residues, which have found their way into the environment through industrial and domestic wastewaters, hospital waste disposal and landfill leachates, are of particular concern due to the widespread use and abuse of these drugs [1,2].

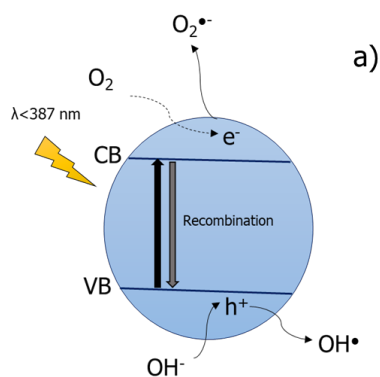
Diclofenac (DCF), an analgesic, nonsteroidal, anti-inflammatory, antirheumatic and antiarthritic compound, is one of the most used pharmaceuticals (approximately 940 tons per year) that has been classified as ecotoxic; hence, it has recently been included on the list of priority pollutants by the European Union [3–5]. Diclofenac possesses acute toxicity in water, even at levels below 100 ppm, and has been reported in drinking water, rivers, hospital waste and groundwater [6–9].

Heterogeneous photocatalysis is an effective advanced oxidation process for eliminating this type of contaminant. The photocatalytic oxidation process for pharmaceuticals in water is based on the generation of very powerful reactive oxygen species (ROS) using semiconductor materials activated by light. In such a process, the photon energy absorbed by the semiconductor generates electron-hole pairs in the bulk of the material. These paired species can either recombine or after migration to the surface, can interact with adsorbed species through redox processes.

Titanium dioxide ( $\text{TiO}_2$ ) is a highly effective semiconductor material that is able to decontaminate water via heterogeneous photocatalysis due to its favorable optical properties, high chemical and thermal stabilities, nontoxicity, commercial availability and low cost [10]. This catalyst generates electron-hole pairs by the absorption of light with a minimum energy of 3.2 eV (corresponding to wavelengths  $\leq 384$  nm); however, this energy is only available in the UV range of the electromagnetic spectrum [11]. The utilization of abundant and freely available solar light for the activation of  $\text{TiO}_2$  is therefore limited to only 4% of the energy reaching the earth surface, although an additional 50% of visible-light energy is potentially available for the activation of  $\text{TiO}_2$  [12]. Several strategies have been implemented to increase the absorption spectrum of  $\text{TiO}_2$  from the UV to the visible region of the solar

spectrum, notably, by doping with elements such as N, S, and C; by coupling with other semiconductors; or by using sensitizing dyes. The latter option is widely used for energy production by photovoltaics [13–21]. Dyes easily adhere to a catalyst's surface and achieve their excited state by the absorption of photons in the visible range of the solar spectrum. Once excited, electrons from the dye's highest occupied molecular orbital (HOMO) are transferred to its lowest unoccupied molecular orbital (LUMO) and subsequently to the conduction band (CB) of  $\text{TiO}_2$  [22] (see Fig. 1). Therefore, the sensitization of  $\text{TiO}_2$  using dyes is a simple and viable technique to absorb a higher fraction of the available solar energy. The dye, in addition to being able to transfer electrons to the catalyst surface under solar irradiation, can also be excited to a triplet state through the absorption of visible light, and subsequently transfer its excess energy to the ground triplet state of oxygen species, generating singlet oxygen by energy transfer or superoxide radical anion by electron transfer [23].

### Photocatalysis with $\text{TiO}_2$



### Dye-sensitized $\text{TiO}_2$

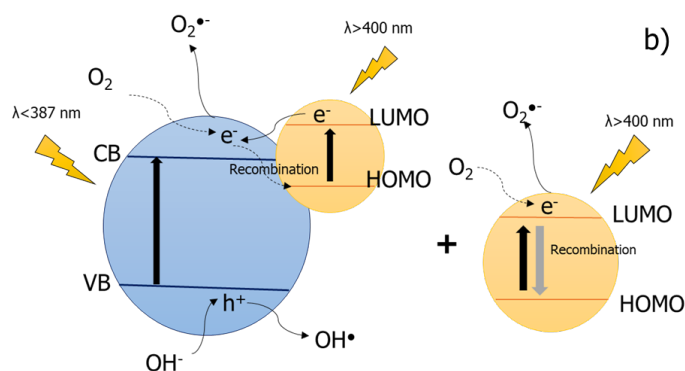


**Fig. 1.** Mechanisms of (a) photocatalysis and (b) the dye-sensitization process. Adapted from Diaz et al. [24].

The injection of electrons into the conduction band (CB) of  $\text{TiO}_2$  results in the formation of a higher concentration of ROS, such as the superoxide anion radical, which in turn, further increase the degradation rate of pollutants compared to that of the conventional photocatalytic process using unmodified  $\text{TiO}_2$ . The dye-sensitization of photocatalysts has been exploited for the degradation of chlorophenol, hydrazine, pesticides and phenol [12,14,25] and even as a means to increase the removal rate of dyes in water, e.g., by the self-sensitization of methyl blue, rhodamine B and other dyes [10,26,27]. Although these laboratory studies have demonstrated the potential of using dyes to absorb visible solar light for photocatalysis, studies of photocatalysis with natural solar radiation at the pilot or industrial scale have not been reported [23,28,29].

In photocatalytic water treatment, the absorption of solar light by the photocatalyst is an important step that determines the overall efficiency of the process. Apart from the intrinsic optical properties of the material, the optimization of the radiation field in photocatalytic reactors is of absolute importance to produce effective harvesting of solar energy, and this task is achieved by the analysis and optimization of the spatial distribution of the local volumetric rate of photon absorption (LVRPA) in the reactor [30–32]. Since the catalyst concentration is often kept constant, the LVRPA is independent of the variable reaction time (or space time) and can be estimated a priori of a full kinetic modeling of the reactor. On the other hand, in dye-sensitized oxidative processes, both the catalyst and dye can absorb solar light, and while the catalyst concentration remains unchanged, the amount of dye adsorbed on the catalyst decreases with time as a result of ROS attack; therefore, the LVRPA in the reactor take a dynamic behavior.

In this study, the dynamic behaviour of the LVRPA and the simultaneous degradation of diclofenac in water by dye-sensitized photocatalysis, under direct solar irradiation, in pilot-

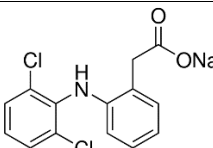
scale compound parabolic collectors (CPCs) was investigated. The degradation kinetics of diclofenac and of the adsorbed dye in the CPCs were modeled considering the dynamic behavior of the LVRPA, and the impact of dye-sensitization was compared with the results obtained using conventional photocatalysis (in the absence of the dye) in the same reactor. The intermediate products produced during the process were investigated by gas chromatography–mass spectrometry and a degradation mechanism is proposed.

## 2. Materials and Methods

### 2.1. Materials

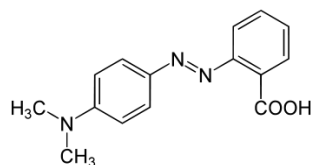
Diclofenac sodium salt (Sigma Aldrich, 98% purity) and methyl red (Merck KGaA, 99.8% w/w purity) sensitizer were used as received. The main properties of diclofenac and methyl red are shown in Table 1. Titanium dioxide Aeroxide® P-25 (80% anatase and 20% rutile crystalline phases; a specific surface area of 50 m<sup>2</sup> g<sup>-1</sup>) was used as the catalyst. Additionally, acetonitrile (Sigma Aldrich, 99.99% analytical grade) and formic acid (Sigma Aldrich, reagent grade ≥95%) were used to prepare the HPLC mobile phase.

Table 1. Diclofenac and methyl red properties.

Compound	CAS	Chemical structure	$\lambda_{\max}$ (nm)	Molecular weight (g mol <sup>-1</sup> )
Diclofenac	15307-79-6		276	318.13

Methyl Red

493-52-7



430

269.30

---

## 2.2. Photoreactor

The experimental tests were performed in pilot-scale CPC photoreactors with identical geometric and hydrodynamic configurations (Supporting Information (SI), Fig. S1). Each reactor consisted of 10 Duran glass tubes (1250 mm in length, 32 mm in external diameter and 1.4 in wall thickness) arranged onto an aluminum involute (reflectance  $\Psi = 0.85$ ) supported by a metal structure. Each reactor (7.7 L irradiated volume) was operated in a recirculation operational mode with a water flow rate of 20 L min<sup>-1</sup> obtained using Iwaki centrifugal pumps (Model MD-55R(T)) with 0.5 hp of nominal power and a recirculation tank with maximum capacity of 60 L. The total irradiated area of each reactor was 1.1 m<sup>2</sup>.

## 2.3. Photodegradation experiments

Each CPC reactor was shielded from solar light prior to the start of an experiment. A 20 L aqueous solution containing dissolved diclofenac (20 mg L<sup>-1</sup>) was initially recirculated in the reactor for 15 min. Then, methyl red dye and TiO<sub>2</sub> were added simultaneously. The slurry suspension was recirculated for an additional 30 min to promote the adsorption of the dye and DCF onto the catalyst surface. Finally, the reactor was exposed to sunlight radiation. Air was constantly injected into the recirculation tank to keep a constant concentration of dissolved oxygen above 80% saturation. All tests were performed under similar conditions of solar radiation at the Solar Photocatalysis Laboratory of the Universidad del Valle, located in Cali (Colombia) (3° 29'N latitude) from September to mid-November, 2015. The intensity

of the solar radiation and the accumulated energy were measured using a radiometer (Delta OHM HD 2102.2) with a UV probe (LP 471) and a visible probe (LP 471 PHOT). The total accumulated energy was  $270 \text{ kJ}\cdot\text{m}^{-2}$  ( $75 \text{ W}\cdot\text{h}\cdot\text{m}^{-2}$ ), of which  $105 \text{ kJ}\cdot\text{m}^{-2}$  ( $29 \text{ W}\cdot\text{h}\cdot\text{m}^{-2}$ ) corresponds to UVA energy. Samples were taken each  $40 \text{ kJ}\cdot\text{m}^{-2}$  ( $10 \text{ W}\cdot\text{h}\cdot\text{m}^{-2}$ ) of UVA energy. A pH meter (ACCUMET®- AB15) was used to measure the pH, which was of 7.2 ( $\pm 0.3$ ). Individual photolysis tests for dye and diclofenac were carried out, and the results are given in supporting information (S.2). The MR and DCF interaction in absence of light was investigated to show that these compounds do not interreact in darkness (See S.3).

## **2.4. Analytical methods**

Different analytical techniques were used to determine the diclofenac degradation, dye concentration and the intermediates produced during the photocatalytic process. High-pressure liquid chromatography (HPLC) using an LC-20AT Shimadzu with a diode array detector (DAD) was employed to quantify the diclofenac concentration at a wavelength of 276 nm. Acetonitrile/formic acid (10 Mm, 70/30 v/v) was used as the mobile phase at a flow rate of 0.8 mL/min for operation in isocratic mode. All injections were 20  $\mu\text{L}$ . The analytical column C-18 (150 mm  $\times$  3.9 mm) developed by Phenomenex was used.

UV-VIS spectrophotometry with a UV-1800 Shimadzu was used to determine the dye concentration in solution at a wavelength of 430 nm. The total organic carbon (TOC) was measured in a TOC-VCPH Shimadzu to analyze the residual carbon of both diclofenac and the dye mixture. The intermediate products of the dye and diclofenac were identified by GC-



MS using a Shimadzu QP2010 PLUS with a UV-Vis G1314A detector, electron bombardment at 70 eV, an injection temperature of 200°C and a selective mass detector.

## **2.5. Mechanism of degradation by dye-sensitization process**

### **2.5.1. Adsorption**

The first step in the photosensitization mechanism is the adsorption of dye and diclofenac on the surface of TiO<sub>2</sub> (Eqs. (1) and (2)), which depends on the compounds' concentrations and on the anchoring group that facilitates the strong binding of dye molecules onto the TiO<sub>2</sub> surface. The presence of a carboxyl group in methyl red aids in the dissociative surface adsorption of the dye onto the surface hydroxyl sites of TiO<sub>2</sub> [12].



### **2.5.2. Photon absorption of TiO<sub>2</sub> and dye**

This step corresponds to the catalyst excitation with UV light and the dye excitation with visible light. These reactions are proportional to the radiation intensity incident on the reactor, both in the UV and visible range of the solar spectrum. During this stage, the electron-hole pair and the triplet state of the dye are generated [12,33–35].

In the dye-sensitization process, a fraction of the dye is adsorbed onto the catalyst surface, and another fraction remains in solution, thus the following events may occur:

- I. The catalyst is activated by the absorption of ultraviolet light, generating an electron-hole pair (Eq. (3)).

II. The dye adsorbed on  $TiO_2$  is excited by energy absorption and transfers an electron to the catalyst's conduction band (Eq. (4)).

III. The dye in solution is excited and transfers an electron to the dissolved oxygen (Eq. (5)).



### 2.5.3. Electron injection

The driving force behind reactions (6) and (7) is the potential difference between the LUMO (lowest unoccupied molecular orbital) of the excited dye and the conduction band of  $TiO_2$ , and generally, these reactions are fast on the order of femtoseconds. The electron injection from the dye to the catalyst occurs at a substantially higher speed than the deactivation of the dye ground state, which is on the order of nanoseconds. Therefore, the efficiency of the electron transfer is approximately 100% [12,33]. The reaction (8) corresponds to the superoxide radical anion generation by electron transfer between the dye in solution and dissolved oxygen [34].



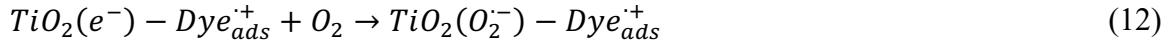
### 2.5.4. Recombination

Reaction (9) represents the electron-hole pair recombination, and this is one of the main causes for the low quantum efficiencies reported in photocatalysis [36]. Reactions (10) and (11) show the generation of the ground state of the dye by recombination of the electron transferred to dissolved oxygen or the electron transferred to the conduction band of TiO<sub>2</sub>, respectively. The latter reaction is 4000-times slower than the electron injection process [12].



#### 2.5.5. Electron trapping

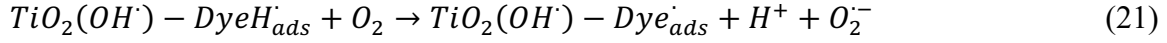
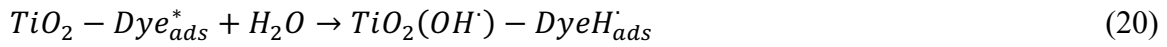
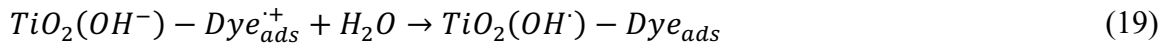
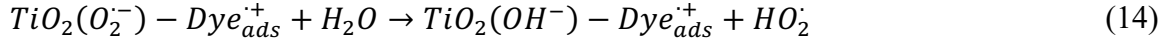
Reactions (12) and (13) represent the superoxide radical formation due to the reaction between molecular oxygen and the electron trapped in the conduction band of TiO<sub>2</sub>, these reactions are limited by the concentration of dissolved oxygen [12,34].



#### 2.5.6. Generation of hydroxyl radical

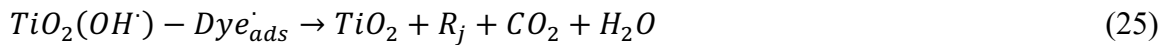
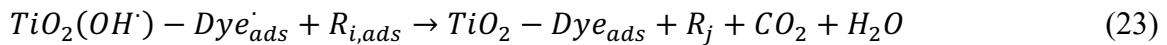
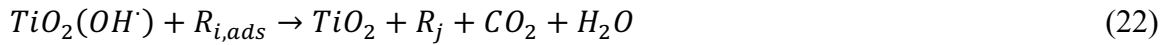
Reactions (14) to (21) indicate the different routes for the generation of oxidizing species. Reactions (14), (15) and (18) represent the hydroperoxyl radical generation by the reaction between the superoxide radical and adsorbed water molecules on the catalyst surface [34,37]. The routes for hydroxyl radical formation in solution and on the catalyst surface are represented by reactions (20) to (24). The typical formation of OH• by heterogeneous photocatalysis is shown in reaction (18), and the reactions (19), (20) and (21) illustrate the

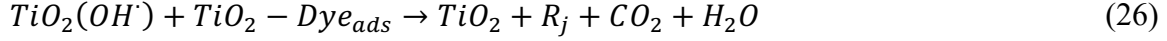
OH• generation by the dye-sensitization process that it also accompanied by dye regeneration [12,34,36]. DyeH<sup>•</sup><sub>ads</sub> is the semi-reduced form of the dye, which is formed by a hydrogen transfer between the triplet excited state of the dye and water [38].



### 2.5.7. Diclofenac and dye degradation

Diclofenac and the dye are simultaneously degraded by hydroxyl radicals adsorbed on the catalyst surface (reactions (22), (23), (25) and (26)) and in solution ((24) and (27)).





## 2.6. Modeling of dye-sensitization process in solar CPC's reactors

### 2.6.1. Kinetic model

To design a reactor or to make a change of scale, a kinetic model that mathematically represents the reaction rate of one or more compounds is necessary. With regards to photocatalytic processes, the reaction rate depends mainly on the catalyst concentration, contaminant concentration and LVRPA or  $e_\lambda^a$ , as described in Eqs. (28-29).

On the other hand, in the dye-sensitization process, the reaction rate of compound  $i$  ( $r_i$ ) is also a function of the dye concentration since the dye absorbs radiation and modifies the LVRPA. Additionally, the dye is an organic substance susceptible to the attack of oxidizing species, which indicates that its degradation must be considered.

$$r_i = f(C_{dye}, C_{cat}, C_i, e_\lambda^a) \quad (28)$$

$$r_{dye} = f(C_{dye}, C_{cat}, C_i, e_\lambda^a) \quad (29)$$

A kinetic model for diclofenac and dye degradation by the dye-sensitization process was formulated using the approach of a pseudo-steady state for all the radical species. The main reaction path considered is the oxidation of organic substances on the catalyst surface, and the assumptions of the model are: *i*) The dye is adsorbed onto the catalyst surface, *ii*) UV absorption of the catalyst free of dye, *iii*) mass transfer limitations are not present, *iv*) species adsorbed on the catalyst surface are in chemical equilibrium, and *v*) the kinetic model is a function of the total charge of  $TiO_2$  (or  $TiO_2$  concentration). This consideration is an effective

approximation because it does not require the introduction of the number of particles ( $Nv$ ), the total surface area ( $Sg$ ), or the particle constant ( $Kp$ ), which are included in the previous models of photocatalysis with  $TiO_2$  [36,39–41]. Furthermore, this approach permits a description of the global performance of the reactions.

The final kinetic rate expressions for diclofenac and methyl red degradations are given by Eqs. (30) and (31), respectively

$$r_{Ri} = - \left( \chi'_1 \frac{0.5 \sqrt{1 - 4\alpha'_1 [TiO_2] \int_{V_R} LVRPA} - 0.5}{[R_i] + k_{ads} [Dye]} + \frac{\chi'_2 \cdot [TiO_2] [Dye] \int_{V_R} LVRPA}{\beta_1 [R_i] + 1} \right) [R_i] \quad (30)$$

$$r_{Dye} = - \left( \chi'_3 \frac{0.5 \sqrt{1 - 4\alpha'_1 [TiO_2] \int_{V_R} LVRPA} - 0.5}{[R_i] + k_{ads} [Dye]} + \frac{\chi'_4 \cdot \int_{V_R} LVRPA}{\beta_1 [R_i] + 1} \right) [Dye] \quad (31)$$

where  $r_{Ri}$  is the rate of diclofenac degradation ( $\text{mol L}^{-1}\text{min}^{-1}$ );  $r_{Dye}$  is the rate of dye degradation ( $\text{mol L}^{-1}\text{min}^{-1}$ );  $[TiO_2]$ ,  $[R_i]$ , and  $[Dye]$  are the concentrations of the catalyst, diclofenac and methyl red, respectively;  $\chi'_1$ ,  $\chi'_2$ ,  $\chi'_3$ ,  $\chi'_4$ ,  $k_{ads}$ ,  $\beta_1$  and  $\alpha'_1$  are the kinetic parameters, which are fitted by coupled optimization methods; and  $\int_{V_R} LVRPA$  represents the average volumetric rate of photon absorption.

The rate expressions were obtained from the mechanism previously described and can be considered a contribution sum of the sensitized and photocatalytic processes. The first term in (Eq. 30) and (Eq. 31) is related to the attack of hydroxyl radicals generated by the reaction between the holes in the valence band and the water adsorbed on the catalyst's surface, i.e., taking into account only the photocatalytic process. The second term considers the attack of radicals species formed by the electron transfer from the dye to the catalyst, which is a product of the dye photon absorption (the development of the model is detailed in the Supporting information S.5).

### 2.6.2. Radiant field

The radiant field in the CPC's reactors under natural solar radiation has been widely studied [30–32]. Colina et al., Mueses et al., and Otalvaro et al. have used the ray tracing technique for drawing the trajectories of solar rays that directly impact the reactor and those that are reflected toward the reactor by the parabolic collectors. In this work, the same methodology was used, and it was assumed that the solar rays are parallel to the vertical direction of the reactor.

From the mechanism, a kinetic expression is obtained for the nonilluminated stages; however, it is necessary to couple this expression to that of the activation stage by calculating the LVRPA or  $e_\lambda^a$ , which represents the number of photons absorbed per unit of time and volume. The LVRPA is described by Eq. (32), and its theoretical determination requires the use of a radiative transfer model.

$$e_\lambda^a(x, t) = \int_{\lambda_{min}}^{\lambda_{max}} \int_{\Omega} \kappa_{\lambda(x)} I_\lambda(x, \Omega) d\Omega d\lambda \quad (32)$$

where  $\kappa_\lambda$  is the volumetric coefficient of absorption for the system and  $I_\lambda$  is the photon irradiance. For an optically transparent solution,  $e_\lambda^a$  is estimated via a radiative transfer model uncoupled to the degradation of reacting species because, in this case, the catalyst is the only component that absorbs and scatters radiation. Therefore, first, the value of  $e_\lambda^a$  is obtained, and then, it is inserted into a kinetics rate laws expression of the water contaminants to obtain the pollutants concentration profile.

On the other hand, in the dye-sensitization process,  $e_\lambda^a$  is a function of the catalyst and dye concentrations since both species can absorb light; therefore, the estimation of  $e_\lambda^a$  cannot be

completely uncoupled from kinetics of the reacting species since the dye is dynamically degraded, which makes the system more complex. The algorithm used in this work for this purpose is provided in Supporting information (S.7).

For sensitized systems, the volumetric coefficient of absorption for the slurry is considered to be the sum of the volumetric coefficient of absorption for the catalyst and volumetric coefficient of absorption for the dye, as shown in Eq. (33).

$$\kappa_{\lambda} = C_{dye}(t)\kappa_{\lambda,dye}^{*} + C_{cat}\kappa_{\lambda,cat}^{*} \quad (33)$$

where  $\kappa_{\lambda,dye}^{*}$  is the dye-specific absorption coefficient for methyl red, which was calculated following the methodology proposed in Villafán et al. and Gr̃ci' and Li Puma [42,43], and  $\kappa_{\lambda,cat}^{*}$  is the TiO<sub>2</sub>-Aeroxide-specific absorption coefficient that is reported in the literature [44].

Another aspect to consider is the variation in  $e_{\lambda}^a$  with environmental conditions. This aspect has been considered by Colina et al. [19] and Otalvaro et al. [32]. In these cases. For the same concentration of catalyst, different values of the LVRPA are obtained due to the temporal variation in the radiation intensity at the solar scale, which has an impact on the reaction kinetics.

A six-flux scattering model (SFM) reformulated for a slurry system where only the catalyst can scattering and both the catalyst and dye can absorb photons was used for calculating the local volumetric rate of photon absorption (LVRPA o  $e_{\lambda}^a$ ) in the CPCs reactors.



$$LVRPA_{(t)} = \frac{I_{0,(t)}}{\lambda_{wcorr} w_{corr} (1 - \gamma)} \left[ \left( w_{corr} - 1 + \sqrt{1 - w_{corr}^2} \right) e^{-\frac{rp}{\lambda_{wcorr}}} \right. \\ \left. + \gamma \left( w_{corr} - 1 - \sqrt{1 - w_{corr}^2} \right) e^{-\frac{rp}{\lambda_{wcorr}}} \right] \quad (34)$$

where  $I_{0,(t)}$  corresponds to the incident solar flux, which changes because of climatic conditions or cloudiness; therefore, it was estimated for each interval of reaction using Eq. (35)

$$I_{0,(t)} = \frac{Q_{ac,(t_2)} - Q_{ac,(t_1)}}{t_2 - t_1} \quad (35)$$

The accumulated radiation ( $Q_{ac}$ ) for each test was measured using a radiometer, as described in *section 2.3*. Details of the calculation of the LVRPA for the dye-sensitized system by the SFM method can be seen in a previous work [24].

The volumetric average of the LVRPA was calculated by Eq. (36):

$$VRPA = \langle LVRPA \rangle_{V_R} = \frac{\int_0^R \int_0^{2\pi} LVRPA(C_{cat}, C_{dye}, r, \theta) r dr d\theta}{\int_0^R \int_0^{2\pi} r dr d\theta} \quad (36)$$

### 2.6.3. Hydrodynamic model

The CPC's reactors operated with turbulent flow to avoid mass transfer limitations and catalyst sedimentation. The fluid dynamic models of these types of reactors are described by Colina et al. and Otalvaro et al. [19,44]:

$$\frac{v_z}{v_{z,max}} = \left( 1 - \frac{r}{R} \right)^{1/n} \quad (37)$$

$$\frac{v_{z,max}}{v_{z,average}} = \frac{(n+1)(2n+1)}{2n^2} \quad (38)$$

$$v_{z,average} = \frac{Q}{\pi R^2} \quad (39)$$

Here,  $n$  is a parameter that can be calculated by:

$$n = 0.41 \sqrt{\frac{8}{f}} \quad (40)$$

where  $f$  is the friction factor and  $Q$  is the flow rate.

All experimental tests were performed with a flow of 20 Lmin<sup>-1</sup> and a Reynolds of 15000 i.e., in the turbulent regimen.

#### **2.6.4. Model implementation and estimation of parameters**

Spyder (Python 3.6.6) was used as the platform for the numerical solution of the coupled differential equations. To obtain semi-intrinsic parameters the geometry of the reactor and the hydrodynamic model were considered. Furthermore, the photon absorption was calculated by the SFM and introduced into the kinetic model.

Partial differential equations formulated represent the material balances in batch CPCs reactors, with recycling for DCF and dye deduced from the application of a continuity equation in the irradiated zone (Eq. (41) and (42)), and the coupling to the recirculation effect in the tank (dark zone of the reactor, Eq. (43) and (44)). This focus permits a description of the performance of the dynamic system as a function of a stable state [45].

Within the simulation process, a random vector of initial values for parameters is defined to start the iterative process required for the fitting of the kinetic parameters to the experimental data and to minimize the objective functions obtained from Eqs. (41) and (42).

The differential equations of the material balances for DCF and the dye in the recirculation tank and inside of the CPC's reactor are solved by coupling the Nelder-Mead algorithms, orthogonal collocation and Runge-Kutta method of the fourth order (RK4).

The material balance for each compound in the CPC's reactors and the mixing tank is expressed as:

$$\frac{\partial C_{R_i}}{\partial t} = -v_z \frac{\partial C_{R_i}}{\partial z} - \left( \chi'_1 \frac{0.5 \sqrt{1 - 4\alpha'_1 [TiO_2] \int_{V_R} LVRPA} - 0.5}{[R_i] + k_{ads}[Dye]} + \frac{\chi'_2 \cdot [TiO_2][Dye] \int_{V_R} LVRPA}{\beta_1 [R_i] + 1} \right) [R_i] \quad (41)$$

$$\frac{\partial C_{dye}}{\partial t} = -v_z \frac{\partial C_{dye}}{\partial z} - \left( \chi'_3 \frac{0.5 \sqrt{1 - 4\alpha'_1 [TiO_2] \int_{V_R} LVRPA} - 0.5}{[R_i] + k_{ads}[Dye]} + \frac{\chi'_4 \cdot \int_{V_R} LVRPA}{\beta_1 [R_i] + 1} \right) [Dye] \quad (42)$$

$$\frac{dC_{R_i,Tank}}{dt} = \frac{1}{\tau_{Tank}} (C_{R_i,Tank}^{in}(t) - C_{R_i,Tank}) \quad (43)$$

$$\frac{dC_{dye,Tank}}{dt} = \frac{1}{\tau_{Tank}} (C_{dye,Tank}^{in}(t) - C_{dye,Tank}) \quad (44)$$

The z coordinate is taken as the maximum gradient direction (DCF and dye), and during the simulation, this parameter was normalized ( $z^* = z / L$ ; L is the CPC reactor length from  $z = 0$  to  $z = L$ ).

The boundary conditions for the reactive system are:

$$C_{R_i \text{ or } dye}(z, t = 0) = C_{R_i \text{ or } dye}^0$$

$$C_{R_i \text{ or } dye,Tank}(z, t = 0) = C_{R_i \text{ or } dye}^0$$

$$C_{R_i \text{ or } dye}(z = 0, t) = C_{R_i \text{ or } dye,Tank}^{out}(t)$$

where  $C_{R_i \text{ or } dye}^0$  is the initial concentration of the dye or diclofenac,  $\tau_{Tank}$  is the residence time, and  $t$  is the time in minutes. In this work, perfect mixing in the recirculation tank was

considered, as well as the concentration at the inlet to the reactor being the same as that at the outlet of the recirculation tank ( $C_{Ri\ or\ dye, Tank}^{out}(t)$ ). The solution to the differential equations (Eq. (43)) and (Eq. (44)) are the conditions of the inlet to the reactor (DCF and the dye, respectively), and the concentration at the reactor output is the same as that at the input to the tank ( $C_{Ri\ or\ dye, Tank}^{in}(t)$ ).

$$\tau_{Tank} \equiv \frac{\tau_R}{\tau_{TK}} = \frac{V_R/Q}{V_{TK}/Q} = \frac{V_R}{V_{TK}} = \frac{L_R/v_{z,average}}{V_{TK}/Q} \quad (45)$$

The total standard deviation (SD) was used to quantify the relative error between the experimental data and the calculated data (Guo et al., 2014). The general SD is calculated as:

$$SD = \sqrt{\frac{1}{N-1} \sum_{i=1}^N \left[ \frac{(C_{Exp, DFC\ or\ Dye} - C_{Cal, DFC\ or\ Dye})}{C_{Exp, DFC\ or\ Dye}} \right]^2} \quad (46)$$

where N is the total number of experimental data and  $C_{Exp, DFC\ or\ Dye}$  and  $C_{Cal, DFC\ or\ Dye}$  are the experimental and calculated concentrations of the species.

### 3. Results and discussion

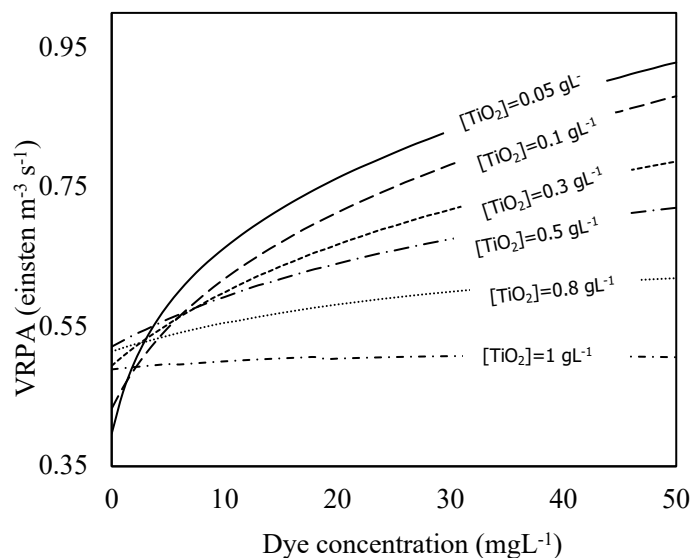
#### 3.1. Radiant energy distribution and photon absorption

Fig. 2 shows the simulated effect of the initial dye concentration on the volumetric rate of photon absorption (VRPA) for different catalyst loadings. Each curve begins with the VRPA achieved only by the photocatalytic system without the dye.

At a low catalyst loading, the system (catalyst and dye) behaves as a homogeneous solution, i.e., increasing the dye concentration enhances considerably the VRPA. However, above 0.5 gL<sup>-1</sup> of catalyst loading, the system behaves as a slurry, and at higher dye concentrations, the

improvement in the VRPA reduces. Even for a catalyst concentration of  $1 \text{ gL}^{-1}$ , the photon absorption is not enhanced by the presence of the dye (this was experimentally verified in Section 3.5).

The results shown in Fig. 2 indicate that at a low catalyst concentration, high values of VRPA can be obtained simply by adding a sensitizing dye to the photocatalytic system. Although the simulation was run until  $50 \text{ mgL}^{-1}$  of dye and the improvement in the VRPA is considerably high for low and middle catalyst loadings, it should be noted that it is not practical to use a dye concentration higher than  $10 \text{ mgL}^{-1}$  of dye. This limitation is not only to achieve a higher photon absorption efficiency but also to ensure the dye does not remain in the effluent after the contaminants are fully removed from the system. Therefore, in this work, 2 and  $4 \text{ mgL}^{-1}$  of dye were used for the experimental tests.



**Fig. 2.** Effect of the catalyst and dye concentrations on the VRPA.

In Fig. 3 the variations in the VRPA for the sensitized and nonsensitized systems as a function of time are presented. The initial dye concentration is fixed at  $4 \text{ mgL}^{-1}$ , and the catalyst

concentrations are 0.1, 0.3, 0.5 and 1 gL<sup>-1</sup>. For the nonsensitized system, the VRPA is constant, which is typical of a photocatalytic process where only the catalyst absorbs light [19,43]. However, the sensitized system presents a dynamic variation of the VRPA, which occurs because of the decrease in the dye concentration, a product of the degradation.

The improvement in the VRPA for the sensitized system at catalyst concentrations of 0.1, 0.3 and 0.5 gL<sup>-1</sup> compared with that for the nonsensitized system is noteworthy. However, at higher catalyst concentrations, the decomposition of the dye becomes greater, and this considerably reduces the VRPA down to its limit, which is given by the photon absorption of the catalyst only. In the sensitized system, a catalyst concentration above of 0.5 gL<sup>-1</sup> decrease the VRPA, hence, the dye becomes another contaminant to be degraded.

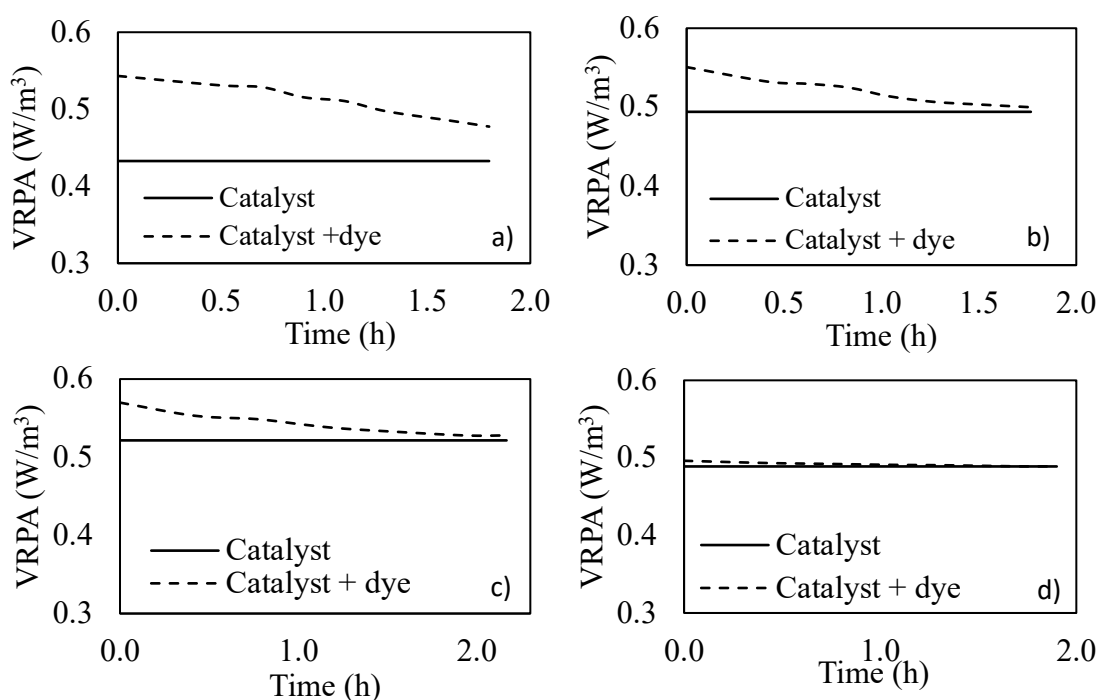
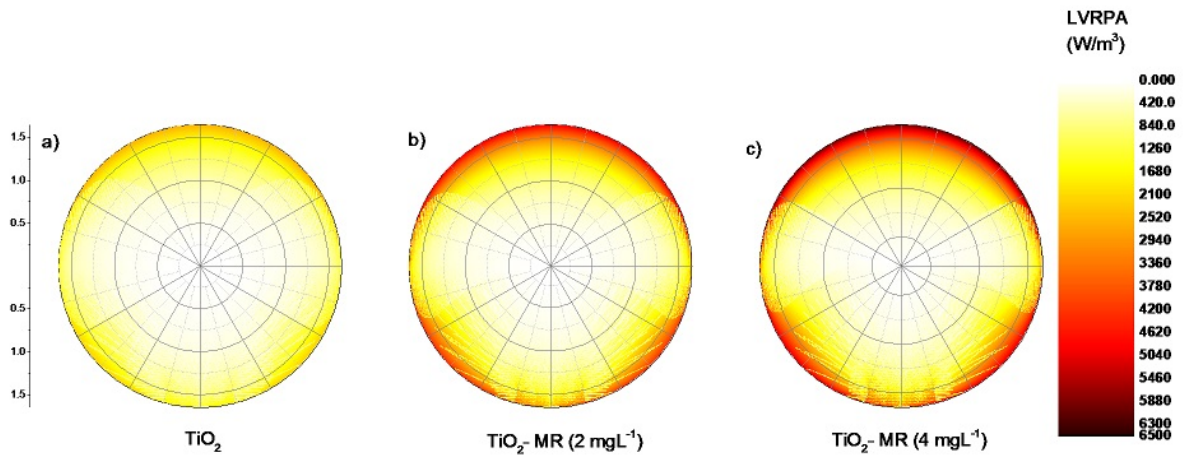


Fig. 3. Variation in the VRPA for sensitized and nonsensitized systems, [Dye<sub>0</sub>] = 4 mgL<sup>-1</sup>. a) [TiO<sub>2</sub>] = 0.1 gL<sup>-1</sup>, b) [TiO<sub>2</sub>] = 0.3 gL<sup>-1</sup> c) [TiO<sub>2</sub>] = 0.5 gL<sup>-1</sup> and d) [TiO<sub>2</sub>] = 1 gL<sup>-1</sup>.

The radiant energy distribution for a transversal circular section of a tube in both sensitized and nonsensitized systems is shown in Fig. 4. It is evident that the sensitized systems exhibit an LVRPA that is substantially higher than that of the nonsensitized system, and it varies with the dye concentration. Colina J et al., Junyi Hou et al. and Otalvaro H et al. [30,32,46] have reported that in photocatalytic systems, increasing the catalyst loading enhances the LVRPA until an optimum point concentration is reached ( $0.5 \text{ gL}^{-1}$  under the present experimental conditions). Nevertheless, as the catalyst concentration is further increased above the optimum, the incident solar flux would not penetrate through the inner areas of the tube, therefore, part of the reactor volume becomes photocatalytically inactive. In the dye-sensitized process, the dye allows a more effective irradiation of the entire reactor volume, as shown in Fig. 4.



**Fig. 4.** LVRPA distributions in CPC reactor for  $0.1 \text{ gL}^{-1}$  of catalyst concentration (a) non-sensitized process, (b) and (c) sensitized process with  $[\text{MR}] = 2 \text{ mgL}^{-1}$  and  $[\text{MR}] = 4 \text{ mgL}^{-1}$  respectively.

### 3.2. Effect of catalyst loading

Further experimental tests were performed at  $\text{TiO}_2$  concentrations of 0.1, 0.3, 0.5 and 1.0  $\text{gL}^{-1}$ , to determine the effect of the catalyst concentration on the degradation of diclofenac. Fig. 5 indicates that the degradation of diclofenac increases with the catalyst concentration. However, at  $\text{TiO}_2$  catalyst loadings above 0.5  $\text{gL}^{-1}$ , the improvement is not significant because similar degradation rates at 0.5 and 1  $\text{gL}^{-1}$  (91.9 and 93.5%, respectively) are obtained. These results are in agreement with those reported by Vinu et al. and Zyoud et al. [10,12]. in laboratory scale reactors. With increasing catalyst concentration, a larger surface area and a higher photon absorption capacity are obtained, which explains the greater degradation of diclofenac at higher concentrations of  $\text{TiO}_2$ . However, it should be noted that the maximum VRPA under the present experimental conditions occurs at a  $\text{TiO}_2$  catalyst loading of 0.5  $\text{gL}^{-1}$  (Fig. 2) and that this corresponds to reaching the maximum degradation of diclofenac.



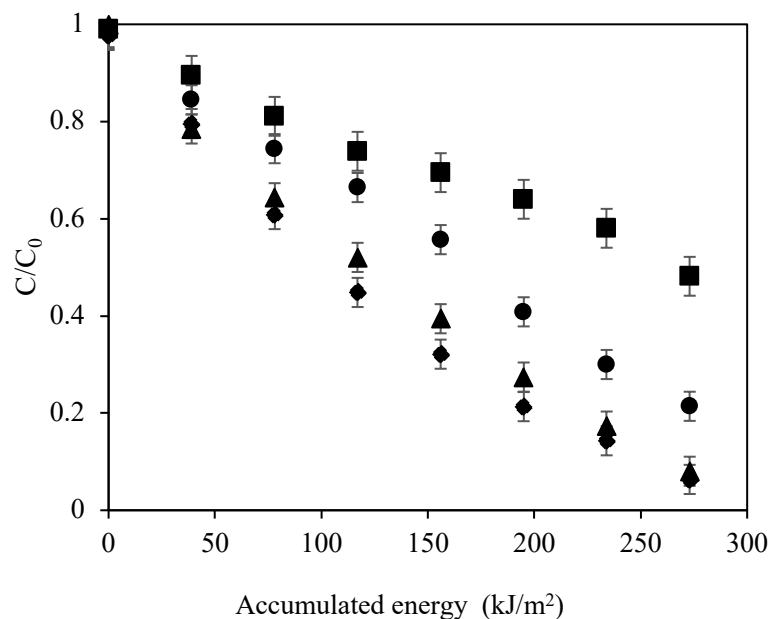


**Fig. 5.** Degradation profiles for 20 mgL<sup>-1</sup> of diclofenac at different catalyst loadings. [MR] = 2 mgL<sup>-1</sup>, (■) [TiO<sub>2</sub>] = 0.1 gL<sup>-1</sup>, (●) [TiO<sub>2</sub>] = 0.3 gL<sup>-1</sup>, (▲) [TiO<sub>2</sub>] = 0.5 gL<sup>-1</sup>, and (◆) [TiO<sub>2</sub>] = 1 gL<sup>-1</sup>.

### 3.3. Effect of initial dye concentration

The effect of the initial dye concentration on the diclofenac degradation was investigated by carrying out tests with 2 and 4 mgL<sup>-1</sup> of methyl red. Fig. 6(a) and 6(b) show the degradation profiles for diclofenac using 0.1 and 1 gL<sup>-1</sup> of TiO<sub>2</sub>, respectively.

In Fig. 6(a), it can be seen that the diclofenac degradation is considerably higher for the dye-sensitized systems, especially at an initial dye concentration of 4 mgL<sup>-1</sup>. Even at a catalyst concentration of 0.1 gL<sup>-1</sup>, an improvement of 44.3% in diclofenac degradation compared to that of the nonsensitized test is obtained. Vinu et al. and Kuo et al. [12,25] have reported

similar results, but these studies are carried out at the laboratory level using artificial solar light.

In contrast of the results mentioned above, Fig. 6(b) shows that with using a high catalyst concentration of  $1.0 \text{ gL}^{-1}$  of  $\text{TiO}_2$ , which is well above the optimum, the effect of the initial dye concentration is negligible. This result can be explained by two main aspects: First, according to the simulation in section 3.1, for a catalyst concentration of  $1.0 \text{ gL}^{-1}$ , the photon absorption does not improve in the sensitized system (Fig. 3d). For this reason, the same diclofenac profiles are obtained for the sensitized and nonsensitized systems. Second, photocatalysis is a nonselective technique; therefore, all the organic molecules in solution are susceptible to degradation, and methyl red competes with diclofenac for the oxidizing species.

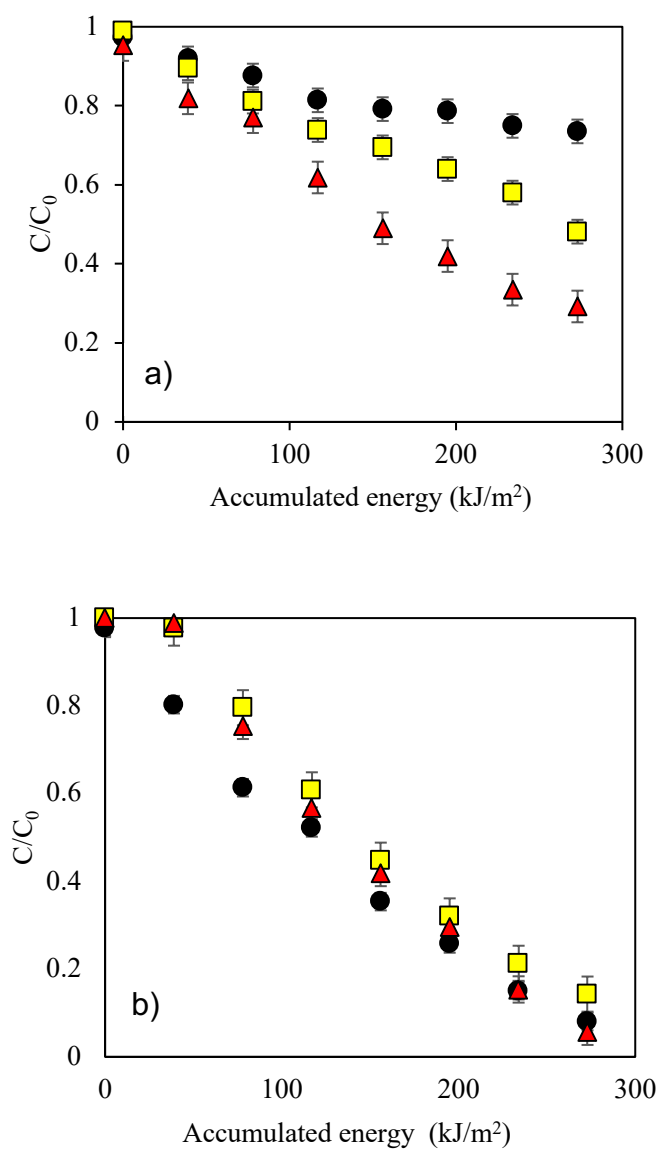


**Fig. 6.** Effect of the initial dye concentration on the diclofenac degradation. a)  $[\text{TiO}_2] = 0.1 \text{ gL}^{-1}$  and b)  $[\text{TiO}_2] = 1 \text{ gL}^{-1}$ . (●) without MR dye, (■)  $[\text{MR}] = 2 \text{ mgL}^{-1}$ , and (▲)  $[\text{MR}] = 4 \text{ mgL}^{-1}$ .

### 3.4. Dye degradation

Fig. 7 illustrates the dye degradation profiles during the dye-sensitization process for different catalyst loadings. The initial points in accumulated energy “zero” correspond to the adsorption of the dye onto the catalyst surface under darkness. It can be seen that the higher the  $\text{TiO}_2$  concentration is, the higher the amount of dye adsorbed over the catalyst, which is result from the higher availability of actives sites.

Methyl red is an azoic dye characterized by having the group  $-(\text{N}=\text{N})-$ , which has chemical inertness and photostability. Due to these characteristics and its anchoring group  $(-\text{COOH})$ , MR was chosen as a sensitizer. However, at industrial or pilot scale, the disposal of the wastewater to an effluent is necessary, so the dye needs to be fully degraded in the effluent. The dye degradation results are: 70% (at  $0.1 \text{ gL}^{-1}$ ), 90% (at  $0.3 \text{ gL}^{-1}$ ), 99% (at  $0.5 \text{ gL}^{-1}$ ) and 99% (at  $1.0 \text{ gL}^{-1}$ ), which suggest that the dye is completely removed once optimal catalyst concentrations of  $0.5 \text{ gL}^{-1}$  and above are used.

The degradation of dye is a key aspect for a possible industrial application of the photocatalysts sensitization process, in either batch and/ or continuous operational mode. The sensitizer dosage depends on the initial concentration of water contaminants, nature of the contaminant, water matrices and the reaction time required. Therefore, it should be possible to use dosing pumps to maintain a high level of radical oxidative species to achieve an optimal rate of photon absorption and fast degradation of water contaminants [47].

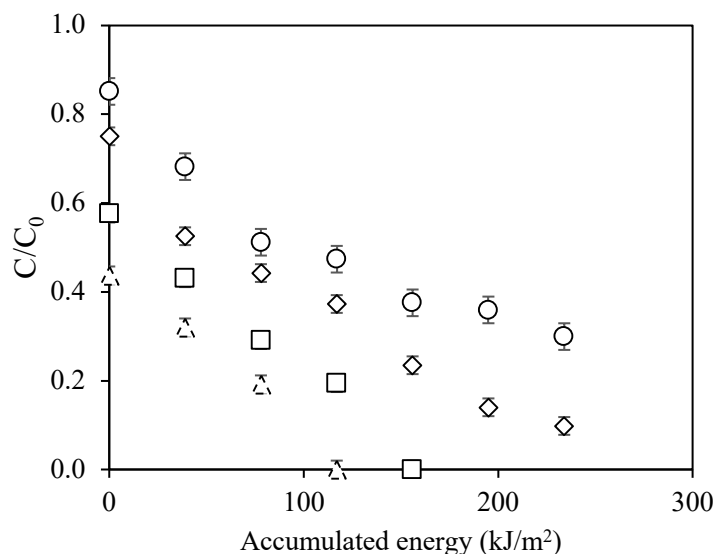


**Fig. 7.** Methyl red degradation during the dye-sensitization process for different  $\text{TiO}_2$  concentrations.  $[\text{DCF}] = 20 \text{ mgL}^{-1}$ ,  $[\text{MR}] = 4 \text{ mgL}^{-1}$ .  $\text{TiO}_2$ : ( $\circ$ )  $0.1 \text{ gL}^{-1}$ , ( $\diamond$ )  $0.3 \text{ gL}^{-1}$ , ( $\square$ )  $0.5 \text{ gL}^{-1}$  and ( $\Delta$ )  $1 \text{ gL}^{-1}$ .

### 3.5. Kinetic modeling of dye sensitized process

The development of intrinsic kinetic models is a very interesting aspect, as it allows for the design of reactors at different scales. Few kinetic models found in the literature describe the behavior of the dye-sensitization process from a mechanistic point of view. Table 2 presents a review of different studies on the water contaminant kinetic expressions and their operating conditions. Wu and Chern have reported a kinetic expression derived from a mechanism for the self-sensitization of methyl blue via the network reduction technique, which depends on the concentrations of the catalyst and dye; to the best of our knowledge, this is the first research regarding a kinetic model about the dye-sensitization process [26]. Kuo W.S. et al. have presented a first-order model for the experimental data fit of carbaryl residual degradation, and in this case, Bengal rose was used as a sensitizer [25]. Chakrabarti S. et al.

have derived a kinetic expression for PVC-film degradation in the presence of Eosin Y as a sensitizer dye, and the kinetic expression considered the UV radiation flux.

R. Vinu et al. have proposed a kinetic expression from a detailed mechanism using a cyclic network technique for the degradation of phenolic compounds in the presence of Eosin Y and fluorescein. The radiation flux was evaluated indirectly through a kinetic constant [12]. Although these models correctly describe the experimental data, they do not consider the simultaneous degradation of the contaminant and dye. Furthermore, the photon absorption of the sensitized system is not evaluated.

In previous work, a kinetic expression for the degradation of diclofenac and acetaminophen by the dye-sensitization process was developed, and the photon absorption was estimated by a six-flux scattering model (SFM). However, this study was performed on the lab-scale, and the simultaneous degradation of the dye was not considered, which influences the photon absorption during the reaction [24].

The kinetic rate law model proposed (Eqs. (30) and (31)) can correctly predict the experimental data of diclofenac and methyl red, as shown in Fig. 8, and this indicates that the elementary reactions in the mechanism correspond to the behavior of the dye-sensitization process.

The most effective removal of both diclofenac and dye occurs at a catalyst concentration of 0.5 g L<sup>-1</sup>, which corresponds to the highest value of the VRPA (see Fig 2) for the concentration of dye used.

Table 2. Kinetic expressions used in the dye-sensitization process

Kinetic expression	Catalyst	Dye	Pollutant	Refs
$r_i = kC_i$	TiO <sub>2</sub>	Bengal rose	Carbaryl	[25]
$r_{PVC} = \frac{2k_1[EY][ZnO][I_{UV}] + 2k_2[ZnO]I_{UV}}{I_f W}$	ZnO	Eosin y	2,4,6-Triphenyl pyrrole hydrogen sulfate	[48]
$r_{ph} = \frac{K_D K_{Ph}[Ph][D][TiO_2]}{K_D[D] + K_{Ph}[Ph]}$	CS TiO <sub>2</sub>	Eosin y	Phenol	[12]
$r_{dye} = \frac{k_4[h\nu][dye][TiO_2]}{1 + k_1[h\nu] + k_2[dye] + k_3[dye][h\nu]}$	TiO <sub>2</sub>	Self-sensitization	Methyl blue	[26]
$r_i = \frac{k_{dye}k_r[R_i][dye][TiO_2]\phi VRPA}{k_{dye}[dye] + k_r[R_i]}$	TiO <sub>2</sub>	Eosin y rhodamine B	Diclofenac acetaminophen	[24]

The semi-intrinsic kinetic constant is shown in supporting information. The total standard deviation (SD) was 0.023, which can be due to the partial oxidation of diclofenac and the dye by other species such as singlet oxygen, the superoxide radical and the triplet state of the dye; although the generation of these species is considered in the mechanism, their direct attack is not regarded. Table 3 presented an analysis of the limiting case of the model and which phenomenon governs the kinetics in each case.

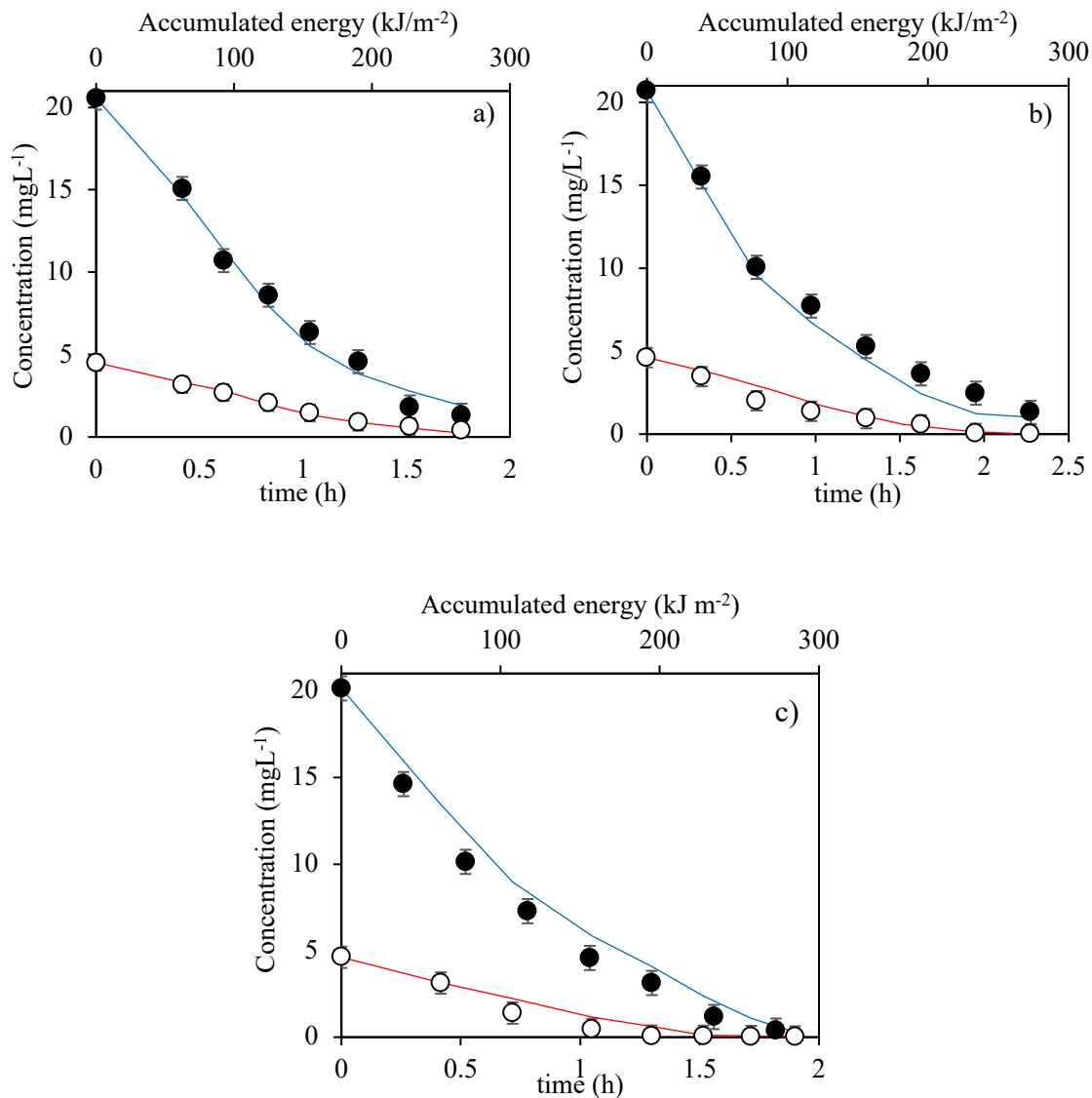


**Fig. 8.** Concentration profiles for the degradation of diclofenac and dye.  $[\text{DCF}_0] = 20 \text{ mg/L}$  and  $[\text{MR}_0] = 4 \text{ mg/L}$ ;  $[(\circ)]$  experimental data of  $[\text{MR}]$ ,  $(\bullet)$  experimental data of  $[\text{DCF}]$ ,  $(—)$  adjusted model of  $[\text{MR}]$  and  $(—)$  adjusted model of  $[\text{DCF}]$ ; a)  $[\text{TiO}_2] = 0.1 \text{ g/L}$ , b)  $[\text{TiO}_2] = 0.3 \text{ g/L}$  and c)  $[\text{TiO}_2] = 0.5 \text{ g/L}$ .



Table 3. Analysis of the limiting cases of the kinetic model

Simplifications	When	Kinetics are controlled by
If $[Dye] = 0$	Heterogeneous photocatalysis.	Oxidizing species generated from catalyst activation.
If $[Dye] \gg R_i$	The oxidizing species generated attack the dye molecules and the sensitized effect on the catalyst decrease.	Self- sensitization process.
If $R_i \gg [Dye]$	The attack to the dye is weak and the dye sensitized process occurs.	Oxidizing species generated from dye and catalyst activation.
If $[Dye] \approx 0$	Dye has been degraded and the sensitized effect on the catalyst does not occurs.	The photon absorption of the catalyst.
If $[Dye] \gg [TiO_2]$	The catalyst particle does not fully activate because dye absorbs all radiation.	The photon absorption of the dye.

### 3.6. Intermediary compounds

Considering the importance of knowing the intermediary compounds of diclofenac and the dye, an identification study of the main degradation products generated during the dye-sensitization process was carried out. Additionally, the possibility of these intermediary compounds reacting to form more complex molecules by an oxidation process was verified.

Organic compounds of the amino type such as 2- [2,6-dichlorophenyl) amino]-5-hydroxyphenylacetic acid and 2,6-dichloro-4-hydroxybenzenamine are evidenced; these products are generated in the oxidation of the diclofenac molecule starting at the amino bond, and their formation is common in most oxidative processes [49]. Hydroxylated species such as 2-Hydroxy-3 - [(9E) -9-octadecenoyloxy] propyl (9E) -9-Octadecenoic are also found because the oxidation process by radical is nonselective [50].

High molecular weight compounds were not evidenced after one hour of treatment, which suggested that the by-products generated by dye and diclofenac degradation do not form stable compounds between them that could become more dangerous, contrary to this a lot of

simple compounds organic such as ketones, alkenes and alkanes were found. Among these, alkanes as Decamethyl Cyclopentane ( $C_{10}H_{30}O_5$ ) and Dodecamethyl Cyclohexane ( $C_{12}H_{36}O_6$ ) were identified (see S.8).

### **3.7. Mineralization of diclofenac and dye.**

Fig. 9 shows the mineralization percentages of the sensitized and non-sensitized tests. In all cases, the dye sensitization process is more efficient in the mineralization process respect to non-sensitized. According to Yan et al., [35] this could be due to the formation of a dye radical cation by electron transfers from LUMO's dye to the conduction band of  $TiO_2$  that react selectively with some organics compounds favoring its mineralization.

It is possible to identify a relationship between the amount of dye and catalyst used, At high catalyst concentration (above  $0.5\text{ gL}^{-1}$ ) the dye is quickly degraded limiting the formation of the dye radical cation and the dye sensitization process, whereas to high dye concentration it competes strongly with the contaminant for the attack of oxidizing species and could remain in solution even after of the treatment, which is undesirable. However, the optimal relationship in this research was  $0.3\text{ gL}^{-1}$  of  $TiO_2$  and  $4\text{ mgL}^{-1}$  of MR where complete mineralization of dye and diclofenac was obtained.

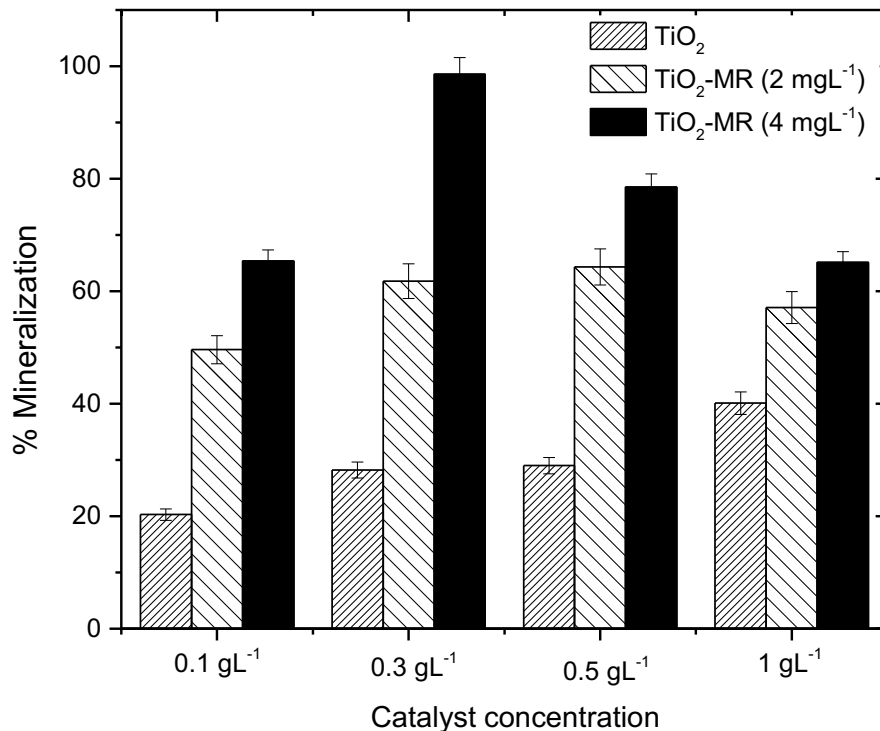


**Fig. 9.** Mineralization of diclofenac and dye for a total accumulated energy of 270 kJm<sup>-2</sup>.

The diclofenac degradation in each case was: (26%) 0.1 gL<sup>-1</sup>, (64%) 0.3 gL<sup>-1</sup>, (87%) 0.5 gL<sup>-1</sup> and (91%) 1 gL<sup>-1</sup> for TiO<sub>2</sub>; (52%) 0.1 gL<sup>-1</sup>, (78%) 0.3 gL<sup>-1</sup>, (92%) 0.5 gL<sup>-1</sup> and (94%) 1 gL<sup>-1</sup> for TiO<sub>2</sub>-MR (2 mgL<sup>-1</sup>) and (71%) 0.1 gL<sup>-1</sup>, (99%) 0.3 gL<sup>-1</sup>, (94%) 0.5 gL<sup>-1</sup> and (99%) 1 gL<sup>-1</sup> for TiO<sub>2</sub>-MR (4 mgL<sup>-1</sup>).

#### 4. Conclusions

This study has demonstrated that the sensitization of TiO<sub>2</sub> with methyl red dye is an efficient approach for the degradation and mineralization of diclofenac, in pilot scale CPCs photoreactors exposed to natural solar radiation. The sensitized system exhibits superior photon absorption efficiency compared to the nonsensitized system, as a result of absorption of visible solar light. However, this effect can be fully appreciated only at catalyst concentrations close to optimum, while excessive catalyst concentrations do not evidence an

apparent improvement of the VRPA and of the mineralization of the contaminant and dye. A sensitization mechanism was proposed and includes the excitation of the catalyst and dye, the electron injection from the dye to the conduction band of the catalyst, the adsorption of both the dye and diclofenac, the recombination of the electron-hole pair and dye radical cation, the generation of oxidizing species and the simultaneous degradation of the dye and diclofenac. The kinetic rate law model formulated in this study was validated with experimental data, and it correctly describes the behavior of the evaluated sensitized system. During the reaction, it was found by GC–MS and TOC analysis that diclofenac and dye simultaneously degradation. Furthermore, simple molecules such as alkanes and alkenes were identified by mass spectroscopy during the degradation of both diclofenac and the dye, which indicate that the dye-sensitization process tends towards complete mineralization. This study has shown the potential of using dye sensitization for the photocatalytic removal of pharmaceuticals and other contaminants of emerging concern in solar, pilot scale photoreactor systems

## **Acknowledgments**

The authors are grateful to Universidad del Valle for the financial support to produce this work through the project 2967. Diaz-Angulo and Lara Ramos thanks to Colombian Administrative Department of Science, Technology and Innovation (COLCIENCIAS) for the Ph.D. Scholarship 647 and 727, respectively. M. A. Mueses thanks Universidad de Cartagena for the financial support. G. Li Puma thanks the support from EU COST Action ES1403UK on New and Emerging Challenges and Opportunities in Wastewater Reuse (NEREUS).

## Appendix A. Supplementary data

Supplementary data to this article can be found online at <https://doi.org/10.1016/j.cej.2019.122520>.

## References

- [1] F.A. Almomani, R.R. Bhosale, M.A.M.M. Khraisheh, A. Kumar, C. Kennes, Mineralization of dichloromethane using solar-oxidation and activated TiO<sub>2</sub> : Pilot scale study, *Sol. Energy*. (2018) 0–1. doi:10.1016/j.solener.2018.07.042.
- [2] Z. Chen, J. Xu, D. Hu, Y. Cui, P. Wu, H. Ge, F. Jia, T. Xiao, X. Li, H. Su, H. Wang, Y. Zhang, Bioresource Technology Performance and kinetic model of degradation on treating pharmaceutical solvent wastewater at psychrophilic condition by a pilot-scale anaerobic membrane bioreactor, *Bioresour. Technol.* 269 (2018) 319–328. doi:10.1016/j.biortech.2018.08.075.
- [3] I. Michael, a. Achilleos, D. Lambropoulou, V.O. Torrens, S. Pérez, M. Petrović, D. Barceló, D. Fatta-Kassinos, Proposed transformation pathway and evolution profile of diclofenac and ibuprofen transformation products during (sono)photocatalysis, *Appl. Catal. B Environ.* 147 (2014) 1015–1027. doi:10.1016/j.apcatb.2013.10.035.
- [4] S. Chong, G. Zhang, Z. Wei, N. Zhang, T. Huang, Y. Liu, Sonocatalytic degradation of diclofenac with FeCeO<sub>x</sub> particles in water, *Ultrason. Sonochem.* 34 (2017) 418–425. doi:10.1016/j.ultsonch.2016.06.023.

- [5] J.M. Monteagudo, A. Durán, I. San Martín, Mineralization of wastewater from the pharmaceutical industry containing chloride ions by UV photolysis of H<sub>2</sub>O<sub>2</sub>/Fe(II) and ultrasonic irradiation, *J. Environ. Manage.* 141 (2014) 61–69.  
doi:10.1016/j.jenvman.2014.03.020.
- [6] B.N. Bhadra, P.W. Seo, S.H. Jung, Adsorption of diclofenac sodium from water using oxidized activated carbon, *Chem. Eng. J.* 301 (2016) 27–34.  
doi:10.1016/j.cej.2016.04.143.
- [7] Y. Wang, H. Liu, G. Liu, Y. Xie, X. Liu, Kinetics for diclofenac degradation by chlorine dioxide in aqueous media: Influences of natural organic matter additives, *J. Taiwan Inst. Chem. Eng.* 56 (2015) 131–137. doi:10.1016/j.jtice.2015.04.015.
- [8] S. Poirier-Larabie, P.A. Segura, C. Gagnon, Degradation of the pharmaceuticals diclofenac and sulfamethoxazole and their transformation products under controlled environmental conditions, *Sci. Total Environ.* 557–558 (2016) 257–267.  
doi:10.1016/j.scitotenv.2016.03.057.
- [9] J. Nisar, M. Sayed, F.U. Khan, H.M. Khan, M. Iqbal, R.A. Khan, M. Anas, Gamma – irradiation induced degradation of diclofenac in aqueous solution: Kinetics, role of reactive species and influence of natural water parameters, *J. Environ. Chem. Eng.* 4 (2016) 2573–2584. doi:10.1016/j.jece.2016.04.034.
- [10] A. Zyoud, N. Zaatar, I. Saadeddin, M.H. Helal, G. Campet, M. Hakim, D. Park, H.S. Hilal, Alternative natural dyes in water purification: Anthocyanin as TiO<sub>2</sub>-sensitizer in methyl orange photo-degradation, *Solid State Sci.* 13 (2011) 1268–1275.  
doi:10.1016/j.solidstatesciences.2011.03.020.

- [11] A. Toumazatou, M.K. Arfanis, P.A. Pantazopoulos, A.G. Kontos, P. Falaras, N. Stefanou, V. Likodimos, Slow-photon enhancement of dye sensitized TiO<sub>2</sub> photocatalysis, *Mater. Lett.* 197 (2017) 123–126. doi:10.1016/j.matlet.2017.03.128.
- [12] R. Vinu, S. Poliseti, G. Madras, Dye sensitized visible light degradation of phenolic compounds, *Chem. Eng. J.* 165 (2010) 784–797. doi:10.1016/j.cej.2010.10.018.
- [13] K. Awasthi, H.Y. Hsu, E.W.G. Diau, N. Ohta, Enhanced charge transfer character of photoexcited states of dye sensitizer on the N719/TiO<sub>2</sub> interface as revealed by electroabsorption spectra, *J. Photochem. Photobiol. A Chem.* 288 (2014) 70–75. doi:10.1016/j.jphotochem.2014.05.001.
- [14] C. Bauer, P. Jacques, a Kalt, Investigation of the interaction between a sulfonated azo dye (AO7) and a TiO<sub>2</sub> surface, *Chem. Phys. Lett.* 307 (1999) 397–406. doi:10.1016/S0009-2614(99)00518-7.
- [15] A. Bianco Prevot, D. Fabbri, E. Pramauro, C. Baiocchi, C. Medana, E. Montoneri, V. Boffa, Sensitizing effect of bio-based chemicals from urban wastes on the photodegradation of azo-dyes, *J. Photochem. Photobiol. A Chem.* 209 (2010) 224–231. doi:10.1016/j.jphotochem.2009.11.020.
- [16] C.A. Castro, A. Centeno, S.A. Giraldo, Iron promotion of the TiO<sub>2</sub> photosensitization process towards the photocatalytic oxidation of azo dyes under solar-simulated light irradiation, *Mater. Chem. Phys.* 129 (2011) 1176–1183. doi:10.1016/j.matchemphys.2011.05.082.
- [17] D. Chatterjee, Effect of excited state redox properties of dye sensitizers on hydrogen production through photo-splitting of water over TiO<sub>2</sub> photocatalyst, *Catal.*

Commun. 11 (2010) 336–339. doi:10.1016/j.catcom.2009.10.026.

- [18] G. Chen, H. Sasabe, X.F. Wang, Z. Hong, J. Kido, A squaraine dye as molecular sensitizer for increasing light harvesting in polymer solar cells, *Synth. Met.* 192 (2014) 10–14. doi:10.1016/j.synthmet.2014.02.018.
- [19] J. Colina-Márquez, F. Machuca-Martínez, G. Li Puma, Photocatalytic mineralization of commercial herbicides in a pilot-scale solar CPC reactor: photoreactor modeling and reaction kinetics constants independent of radiation field., *Environ. Sci. Technol.* 43 (2009) 8953–60. doi:10.1021/es902004b.
- [20] I. Kondratyeva, Ł. Orze, I. Kobasa, A. Doroshenko, W. Macyk, Materials Science in Semiconductor Processing Photosensitization of titanium dioxide with 4'-dimethylamino fl avonol, 42 (2016) 62–65.
- [21] A. Yarahmadi, S. Sharifnia, Dye photosensitization of ZnO with metallophthalocyanines (Co, Ni and Cu) in photocatalytic conversion of greenhouse gases, *Dye. Pigment.* 107 (2014) 140–145. doi:10.1016/j.dyepig.2014.03.035.
- [22] M.R. Narayan, Review: Dye sensitized solar cells based on natural photosensitizers, *Renew. Sustain. Energy Rev.* 16 (2012) 208–215. doi:10.1016/j.rser.2011.07.148.
- [23] J. Diaz-Angulo, A. Arce-Sarria, M. Mueses, A. Hernandez-Ramirez, F. Machuca-Martinez, Analysis of two dye-sensitized methods for improving the sunlight absorption of TiO<sub>2</sub> using CPC photoreactor at pilot scale, *Mater. Sci. Semicond. Process.* 103 (2019) 104640. doi:10.1016/J.MSSP.2019.104640.
- [24] J. Diaz-Angulo, I. Gomez-Bonilla, C. Jimenez-Tohapanta, M. Mueses, M. Pinzon, F. Machuca-Martinez, Visible-light activation of TiO<sub>2</sub> by dye-sensitization for



degradation of pharmaceutical compounds, *Photochem. Photobiol. Sci.* 18 (2019) 897–904. doi:10.1039/c8pp00270c.

- [25] W.S. Kuo, Y.H. Chiang, L.S. Lai, Solar photocatalysis of carbaryl rinsate promoted by dye photosensitization, *Dye. Pigment.* 76 (2008) 82–87.  
doi:10.1016/j.dyepig.2006.08.015.
- [26] C.H. Wu, J.M. Chern, Kinetics of photocatalytic decomposition of methylene blue, *Ind. Eng. Chem. Res.* 45 (2006) 6450–6457. doi:10.1021/ie0602759.
- [27] M. Rani, S.K. Tripathi, Electron transfer properties of organic dye sensitized ZnO and ZnO/TiO<sub>2</sub> photoanode for dye sensitized solar cells, *Renew. Sustain. Energy Rev.* 61 (2016) 97–107. doi:10.1016/j.rser.2016.03.012.
- [28] E.-T. Yun, H.-Y. Yoo, W. Kim, H.-E. Kim, G. Kang, H. Lee, S. Lee, T. Park, C. Lee, J.-H. Kim, J. Lee, Visible-light-induced activation of periodate that mimics dye-sensitization of TiO<sub>2</sub>: Simultaneous decolorization of dyes and production of oxidizing radicals, *Appl. Catal. B Environ.* 203 (2017) 475–484.  
doi:10.1016/j.apcatb.2016.10.029.
- [29] P. Chowdhury, S. Athapaththu, A. Elkamel, A.K. Ray, Visible-solar-light-driven photo-reduction and removal of cadmium ion with Eosin Y-sensitized TiO<sub>2</sub> in aqueous solution of triethanolamine, *Sep. Purif. Technol.* 174 (2017) 109–115.  
doi:10.1016/j.seppur.2016.10.011.
- [30] J. Colina-Márquez, F. Machuca-Martínez, G.L. Puma, Radiation absorption and optimization of solar photocatalytic reactors for environmental applications, *Environ. Sci. Technol.* 44 (2010) 5112–5120. doi:10.1021/es100130h.

- [31] M.A. Mueses, F. Machuca-Martinez, A. Hernández-Ramirez, G. Li Puma, Effective radiation field model to scattering – Absorption applied in heterogeneous photocatalytic reactors, *Chem. Eng. J.* 279 (2015) 442–451. doi:10.1016/j.cej.2015.05.056.
- [32] H.L. Otálvaro-Marín, M. Angel Mueses, J.C. Crittenden, F. Machuca-Martinez, Solar Photoreactor Design by the Photon Path Length and Optimization of the Radiant Field in a TiO<sub>2</sub>-based CPC Reactor, *Chem. Eng. J.* 315 (2017) 283–295. doi:10.1016/j.cej.2017.01.019.
- [33] J. He, J. Zhao, T. Shen, H. Hidaka, N. Serpone, Photosensitization of Colloidal Titania Particles by Electron Injection from an Excited Organic Dye–Antennae Function, *J. Phys. Chem. B.* 101 (1997) 9027–9034. doi:10.1021/jp971550v.
- [34] J.C. Yu, Y. Xie, H.Y. Tang, L. Zhang, H.C. Chan, J. Zhao, Visible light-assisted bactericidal effect of metalphthalocyanine-sensitized titanium dioxide films, *J. Photochem. Photobiol. A Chem.* 156 (2003) 235–241. doi:10.1016/S1010-6030(03)00008-X.
- [35] J. Yang, C. Chen, H. Ji, W. Ma, J. Zhao, Mechanism of TiO<sub>2</sub>-assisted photocatalytic degradation of dyes under visible irradiation: Photoelectrocatalytic study by TiO<sub>2</sub>-film electrodes, *J. Phys. Chem. B.* 109 (2005) 21900–21907. doi:10.1021/jp0540914.
- [36] O.M. Alfano, I. Cabrera, A.E. Cassano, Photocatalytic Reactions Involving Hydroxyl Radical Attack I. Reaction Kinetics Formulation with Explicit Photon Absorption Effects, 379 (1997) 370–379.
- [37] J. Zhao, C. Chen, W. Ma, Photocatalytic Degradation of Organic Pollutants Under

Visible Light Irradiation, *Top. Catal.* 35 (2005) 269–278. doi:10.1007/s11244-005-3834-0.

- [38] M. Gmurek, M. Olak-Kucharczyk, S. Ledakowicz, Photochemical decomposition of endocrine disrupting compounds – A review, *Chem. Eng. J.* 310 (2017) 437–456. doi:10.1016/j.cej.2016.05.014.
- [39] M. a. Mueses, F. MacHuca-Martínez, Modelo Matemático para Estimación de Eficiencias Fotónicas No-Intrínsecas en Reacciones Fotocatalíticas Heterogéneas, *Inf. Tecnol.* 23 (2012) 43–50. doi:10.4067/S0718-07642012000300006.
- [40] C.S. Zalazar, R.L. Romero, C.A. Martín, A.E. Cassano, Photocatalytic intrinsic reaction kinetics I: Mineralization of dichloroacetic acid, *Chem. Eng. Sci.* 60 (2005) 5240–5254. doi:10.1016/j.ces.2005.04.050.
- [41] C.S.T.A.D.F. OLLIS, Photocatalytic Degradation of Organic Water Contaminants: Mechanisms Involving Hydroxyl Radical Attack, *J. Geogr. Sci.* 18 (2008) 95–106. doi:10.1007/s11442-008-0095-4.
- [42] H.I. Villafán-Vidales, S.A. Cuevas, C.A. Arancibia-Bulnes, Modeling the Solar Photocatalytic Degradation of Dyes, *J. Sol. Energy Eng.* 129 (2007) 87. doi:10.1115/1.2391255.
- [43] I. Grčić, G. Li Puma, Six-flux absorption-scattering models for photocatalysis under wide-spectrum irradiation sources in annular and flat reactors using catalysts with different optical properties, Elsevier B.V., 2017. doi:10.1016/j.apcatb.2017.04.014.
- [44] H.L. Otálvaro-Marín, M.A. Mueses, F. Machuca-Martínez, Boundary layer of photon absorption applied to heterogeneous photocatalytic solar flat plate reactor

design, *Int. J. Photoenergy*. 2014 (2014). doi:10.1155/2014/930439.

- [45] H.L. Otálvaro-Marín, F. González-Caicedo, A. Arce-Sarria, M.A. Mueses, J.C. Crittenden, F. Machuca-Martinez, Scaling-up a heterogeneous H<sub>2</sub>O<sub>2</sub>/TiO<sub>2</sub>/solar-radiation system using the Damköhler number, *Chem. Eng. J.* 364 (2019) 244–256. doi:10.1016/j.cej.2019.01.141.
- [46] J. Hou, Q. Wei, Y. Yang, L. Zhao, Experimental evaluation of scattering phase function and optimization of radiation absorption in solar photocatalytic reactors, *Appl. Therm. Eng.* 127 (2017) 302–311. doi:10.1016/j.applthermaleng.2017.08.046.
- [47] J. Diaz-Angulo, J. Porras, M. Mueses, R. Torres-Palma, A. Hernandez-Ramirez, F. Machuca-Martinez, Coupling of heterogeneous photocatalysis and photosensitized oxidation for diclofenac degradation: role of the oxidant species, *J. Photochem. Photobiol. A Chem.* (2019) 112015. doi:10.1016/j.jphotochem.2019.112015.
- [48] S. Chakrabarti, B. Chaudhuri, S. Bhattacharjee, P. Das, B.K. Dutta, Degradation mechanism and kinetic model for photocatalytic oxidation of PVC-ZnO composite film in presence of a sensitizing dye and UV radiation, *J. Hazard. Mater.* 154 (2008) 230–236. doi:10.1016/j.jhazmat.2007.10.015.
- [49] P. Calza, V.A. Sakkas, C. Medana, C. Baiocchi, A. Dimou, E. Pelizzetti, T. Albanis, Photocatalytic degradation study of diclofenac over aqueous TiO<sub>2</sub> suspensions, *Appl. Catal. B Environ.* 67 (2006) 197–205. doi:10.1016/j.apcatb.2006.04.021.
- [50] A.D. Coelho, C. Sans, A. Agüera, M.J. Gómez, S. Esplugas, M. Dezotti, Effects of ozone pre-treatment on diclofenac: Intermediates, biodegradability and toxicity assessment, *Sci. Total Environ.* 407 (2009) 3572–3578.

doi:10.1016/j.scitotenv.2009.01.013.